

of Nonlinear Optical IFWM Impairments in Optical Fiber by Modeling 40 Gb/s Transimpedance Amplifier

Muhammed S. Hameed

Department of Physics

College of Science

University of Mosul

E-mail: mohamed.subhyl@yahoo.com

(Received 14/ 11 / 2011 ; Accepted 12 / 3 / 2012)

ABSTRACT

A suppression of nonlinear optical Intra-Channel Four Wave Mixing (IFWM) induced phase and amplitude noise in optical fiber is reported by simulation. A 40 Gb/s transimpedance amplifier (TIA) circuit was investigated for this purpose. Circuit components were modeled under thermal conditions of 30°C. Using 81 kΩ nonlinear feedback resistor R_{TIA} , an optimal Minimum Noise Figure (MNF) of 1.758 dB was achieved. A 1.760 dB of MNF is reported when R_{TIA} value changes to 80 kΩ. However, when an IFWM-induced phase and amplitude combined noise is applied at the TIA input with a magnitude of 19.081 dB, it was effectively suppressed under the influence of TIA input impedance Z_{in} of 19914 Ω which lead to IFWM combined noise of 14.55 dB in a decreasing pattern at TIA output. An $|S_{21}|$ simulated measurement showed a gain of 10.15 dB.

Keywords: IFWM, 40 Gb/s TIA, Nonlinear Optics, Noise Suppression.

/ 40

/ 40

30

() 81

80 1.758 dB

) 1.760 dB

19.081 dB

(

14.55 dB

19914

.10.15 dB |S₂₁|

INTRODUCTION

Optical fiber transmission systems are subject to impairments by Intra-Channel Four-Wave Mixing (IFWM), a form of nonlinear Inter-Symbol Interference (ISI) resulting from the interaction of Kerr nonlinearity and chromatic dispersion (Lau *et al.*, 2008). Nonlinear effects impair the transmitted signal severely over high-speed optical fiber channel, and hence became the main obstacle for long-distance and high quality signal transmission. Research activities for dealing with nonlinearity mainly were dispersion management technologies (Kumar *et al.*, 2002) (Yamamoto *et al.*, 2000) (Morita *et al.*, 1999), or amplification technologies (Hirooka and Ablowitz, 2002) depending on the loss compensation and signal power amplification. Suppression of IFWM nonlinear effects was achieved using optical pulse position modulation (Linghao and Takala, 2003).

A phase-modulated pulse trains in a single-channel system can be transmitted into a fiber. The signal at the transmitter is given by (Lau *et al.*, 2008).

$$E(0,t) = \sum_k x_k u(0,t - kT) = \sum_k x_k u_k \dots\dots\dots (1)$$

where $x_k = \{e^{j2\pi/M}, e^{j4\pi/M} \dots\dots\dots e^{j2\pi}\}$ are the M -ary phase-modulated signals, $u(z,t)$ is the pulse shape, and T is the symbol period. Signal propagation in optical fiber is described by the nonlinear Schrodinger Equ (Agrawal, 2002):

$$\frac{\partial E}{\partial z} - \frac{j\beta_2(z)}{2} \frac{\partial^2 E}{\partial t^2} + \frac{\partial(z)}{2} E = j\gamma(z)|E|^2 E \dots\dots\dots (2)$$

β_2 is the chromatic dispersion parameter and γ which is the nonlinear coefficient. The first-order perturbation theory can be used to approximate the solution of the nonlinear Schrodinger Equ, in which the transmitted signal can be decomposed (Mecozzi, *et al* 2000):

$$E \approx E^{(l)} + \Delta E = \sum_k x_k u_k^l + \Delta u_k \dots\dots\dots (3)$$

Where $E^{(l)}$ is the linear solution of Equation 2, while ΔE is the nonlinear perturbation. The perturbation term satisfies (Lau *et al.*, 2008):

$$\frac{\partial \Delta E}{\partial z} - \frac{j\beta_2(z)}{2} \frac{\partial^2 \Delta E}{\partial t^2} + \frac{\alpha(z)}{2} \Delta E = j\gamma(z)|E^{(l)}|^2 E^{(l)} = j\gamma(z) \sum_{l,m,p} x_l x_m x_p^* u_l^l u_m^l u_p^l \dots\dots\dots (4)$$

With high local dispersion, the terms in the right hand side of Equation 4 that contribute to Δu_k are those with $l + m - p = k$ and therefore, the nonlinear signal perturbations are termed IFWM. The nonlinear perturbation to a pulse $u_0^{(l)}$ originate from Equation 4 is:

$$j\gamma \sum_{l,m} x_l x_m x_{l+m}^* u_l^{(l)} u_m^{(l)} u_{l+m}^{(l)*}$$

$C'_{l,m}$ can be assumed to be the solution to by linearity [Lau, *et al* 2008]:

$$\frac{\partial C'_{l,m}}{\partial z} - \frac{j\beta_2(z)}{2} \frac{\partial^2 C'_{l,m}}{\partial t^2} + \frac{\alpha(z)}{2} C'_{l,m} = j\gamma(z) u_l^{(l)} u_m^{(l)} u_{l+m}^{(l)*} \dots\dots\dots(5)$$

The overall nonlinear perturbations is then $\Delta u_0 = \sum_{l,m} C'_{l,m}(t)$. If $u_0^{(s+x)}$ is denoted as the collective nonlinear deterministic perturbations, the IFWM-induced phase noise can be approximated as [Lau, *et al* 2008]:

$$\varphi_0(t) \approx \sum_{l,m \neq 0} \text{Im} \left\{ \frac{x_l x_m x_{l+m}^* C'_{l,m}(t)}{x_0 (u_0^l + u_0^{(s+x)})} \right\} = \sum_{l,m \neq 0} \text{Im} \{ x_l x_m x_{l+m}^* x_0^* C_{l,m} \} \dots\dots\dots (6)$$

And the IFWM-induced amplitude noise normalized with respect to the signal amplitude is:

$$\Delta r_0(t) = \sum_{l,m \neq 0} \text{Re} \{ x_l x_m x_{l+m}^* x_0 C_{l,m} \} \dots\dots\dots (7)$$

So, the correlation between IFWM-induced phase and amplitude noises is given by:

$$E[\varphi_0(t)\Delta r_0(t)] = E \left[\sum_{l,m \neq 0} \text{Im} \{ AC_{l,m} \} \sum_{l,m \neq 0} \text{Re} \{ AC_{l,m} \} \right] \dots\dots\dots(8)$$

in which $A = x_l x_m x_{l+m}^* x_0^*$.

A 40 Gb/s transimpedance amplifier (TIA) has not yet been considered for suppression of IFWM-induced noise (ghost pulses) accompanying main optical pulse and exiting the fiber. In fact, TIA configuration has never been considered before for processing IFWM-induced noise. That is because noise cancellation techniques were not advanced enough to deal with this problem. The importance of IFWM suppression becomes clear at high data bit rates alongside other nonlinear optical impairments such as self phase modulation and cross talk that need to be suppressed in an optical fiber. The transformation from optical domain (IFWM-induced noise) in an optical fiber to an ac electrical current (electronic domain) does happen when an optical pulse is incident on a photodiode and an electrical current is generated at the input of transimpedance amplifier (TIA). The TIA then converts this electrical current into amplified voltage swing at its output. A Microwave Office program was used to simulate the operation of TIA circuit.

Nonlinear effects impair the transmitted signal severely over high-speed optical fiber channel, and hence became the main obstacle for long-distance and high-quality signal transmission (Linghao and Takala, 2003).

RESULTS AND DISCUSSION

1. TIA Design Analysis

A. Transfer Function

The transfer function of basic schematic of Fig 1 was envisaged according to similar concept stated in already published result (Groenveld, 2010). Although that, in this work, a capacitor C in parallel with feedback “nonlinear” resistor R_{TIA} is taken into account when transfer function (transimpedance gain) is worked out and it is given as follows:

$$\frac{V_{out}}{i_{in}} = \frac{As + B}{as^2 + bs + c} \dots\dots\dots (9)$$

where,

$$\begin{aligned} A &= Z_L R_{TIA} C(g_m Z_{in} - 1) \\ B &= Z_L [g_m (Z_{in} + R_{TIA}) - 1] \\ a &= Z_{in} R_{TIA} C_{in} C \\ b &= R_{TIA} C(g_m Z_L + 1) + C_{in} (Z_{in} + R_{TIA}) \\ c &= g_m Z_L + 1 \end{aligned}$$

g_m is the transistor transconductance measured in Siemens. A zero pole was deduced from Equ 9 as indicated:

$$s = - \frac{g_m (Z_{in} + R_{TIA}) - 1}{R_{TIA} C(g_m Z_{in} - 1)} \dots\dots\dots (10)$$

in which a calculated value showed that $s = - 20.78 \times 10^9$ as $s = j\omega$ where g_m is the transconductance of the common-source configured Angelov (HEMT) Transistor M₁ model (Angelov, 1996). C_{in} is the equivalent input capacitance of TIA as it is within Twin T notch filter at the input. Load impedance $Z_L = R_L / (R_L C_L s + 1)$ and was found to be $|Z_L| = 110.2$ kΩ, while $Z_{in} = 19914 \Omega$ at 40 GHz (measured in simulation) as the input impedance of the TIA and it is the Twin T notch filter total impedance. R_{TIA} was set at a range of 80 kΩ - 81 kΩ. The equivalent passive circuit of R_{TIA} is given in Fig 2 for which the R_{TIA} IV characteristics are illustrated in Equation 11. The IV characteristics are only for the nonlinear resistor R_{TIA} given in the Microwave Office program. The R_{TIA} is assumed by the program to be nonlinear that follows Equation 11, while the two diodes are reverse biased to isolate the earth connection from the actual R_{TIA} resistor.

$$I(V) = \frac{1}{R} \left(V + \frac{1}{2} P V^2 + \frac{1}{3} P_1 V^3 + \dots \right) \dots\dots\dots (11)$$

where P and P₁ are vectors of polynomial coefficients which were set at 1. Setting these vectors at 1 is to have the R_{TIA} resistor behaves in a Taylor Series configuration.

In addition to the zero pole, two complex poles were established using the formula $s = [(- b \pm \text{sqrt}(b^2 - 4ac)) / 2a]$ of the denominator of Equation 9, in which calculated imaginary

values are $s = -3 \times 10^6$ and -9.84×10^9 . A transimpedance gain of $40.82 \text{ dB}\Omega$ is obtained, once a $100 \mu\text{A}$ is applied as TIA input, by which a voltage swing of 0.011V is achieved at the output. The TIA electrical gain may be considered moderate at first glance, however, given the thermal conditions of 30°C for main circuit components (*i.e* resistors and transistor models) as thermal sources, it may have reached its maximum possible value.

B. Noise Cancellation

A noise cancellation process takes place in a virtual ground node between Z_{in} and $(R_{\text{TIA}} \parallel 1/Cs)$ in which a feedback resistor is effectively in place, $R_F = Z_{\text{in}} + (R_{\text{TIA}} \parallel 1/Cs)$. This virtual ground node has two functions. The first is to thermally cancel noise and is located between R_{TIA} and Z_{in} , while the other one is located between $(1/Cs)$ and Z_{in} which is responsible for cancelling (*i.e* suppressing) IFWM combined noise of phase and amplitude. The value of R_F was calculated (frequency domain) and found to equal $20.5 \text{ k}\Omega$. According to already published result with small signal model (Groenveld, 2010), a noise subtraction does happen in which the input referred noise of TIA corresponds to a value of $-R_{\text{TIA}}$ as the minus sign indicates that by increasing R_{TIA} , the input referred noise is decreased. That concept may be true in terms of thermal noise cancellation, however, as it will be seen in IFWM-Induced Noise Section that IFWM-induced noise is not affected by R_{TIA} value, instead it will be influenced by TIA input impedance Z_{in} and that is mainly true due to the virtual ground node between $(1/Cs)$ and Z_{in} . Capacitances C_2 , C_3 and C_4 in Fig 1 could have been reduced even further to fF level, however, it becomes at the expense of overall circuit gain and may not necessarily maintain close matching between noise bandwidth (IFWM in this case) and TIA bandwidth. Hence, the closest matching possible is shown in Table 1.

Table 1: comparison with already published work (Groenveld, 2010)

Value	This Work	Published Work (Groenveld, 2010)
Z_L	$ Z_L = 110.2 \text{ k}\Omega$ $R_F = 20.5 \text{ k}\Omega$ $1/g_m = 20 \text{ k}\Omega$ $Z_L > R_F$ $Z_L > 1/g_m$	- - - $Z_L \gg R_F$ $Z_L \gg 1/g_m$
Z_{in}	19914 Ω Twin T Notch	R_{F1} Resistor
R_{out} of Transistor M_2	$L_{1s} \parallel (1/C_{1s}) = 329 \Omega$	102 Ω Resistor
R_{TIA}	80 $\text{k}\Omega$ - 81 $\text{k}\Omega$ Nonlinear Resistor	R_{F2} (asymmetric) Resistor
Data Rate	40 Gb/s	5.2 Gb/s
TIA Bandwidth	$(g_m Z_L + 1)/C_{\text{in}}(R_F + Z_L)$	$1/(Z_{\text{in}} C_{\text{in}})$
IFWM Noise Bandwidth	$(g_m Z_L + 1)/C_{\text{in}} [(Z_{\text{in}} \parallel (1/Cs) + Z_L)]$	Not Related
Transistor M_1	Angelov (HEMT) (Angelov, 1996)	NMOS
Transistor M_2	Statz (GaAs FET) (Statz, 1987)	PMOS
Group Delay (GD)	0.00098 ns	-
Operating Temp.	30 $^\circ\text{C}$	-

The TIA circuit stability gives a good indication into how functioning is the noise cancellation process. A voltage controlled current source Statz transistor M_2 model (Statz, 1987) is embedded with $(L_{1s} \parallel (1/C_{1s}))$ load that determines how stable is the TIA. Fig 3 shows that the electronic circuit is conditionally stable ($K < 1$) at 40 Gb/s with a strict condition that the real part of Z_{21} parameter is actually below zero which happened to be the case of -6.37 dB.

The idea that the feedback resistor thermal noise dominates the front end noise, and hence the electrical sensitivity being proportional to $1/\sqrt{R_{TIA}}$ can be compromised due to the virtual ground node between R_{TIA} and Z_{in} , especially for a moderately large value of R_{TIA} . Therefore, a form of adaptive nonlinear feedback resistor is exactly what applies to R_{TIA} in which its dynamic range is extended to make it adapt to the input signal strength. Without the virtual ground node, a shunt resistor can be connected in parallel with R_{TIA} in order to extend the TIA dynamic range (adaptive transimpedance), however, this process may not be useful given the need for noise cancellation (Sackinger, 2005).

C. Design Comparison

A comparison in TIA design with already published work (Groenveld, 2010) is illustrated in Table I. There are major differences that involve design consideration at no parasitic capacitance (at this stage). In this work, a twin T notch filter, values of Z_L in relation to R_F and $1/g_m$, TIA bandwidth, types of high-speed transistors, Statz transistor model load and nonlinear resistor form are all exclusively set up. Angelov Transistor M_1 transconductance g_m was calculated and found to have the magnitude of around 5×10^{-5} S, in which $1/g_m$ value is given in Table I. The Angelov model do replace the NMOS transistor, while the Statz model replaces the PMOS transistor. They are by no means equivalent to NMOS and PMOS transistors respectively.

Using the normalized value of ω/ω_n , for which ω_n is the frequency of operation (40 GHz), while ω is the sweeping frequency (*i.e* from 1 GHz up to 40 GHz), the TIA group delay (GD) is shown in Fig 4. The lowest GD value does occur at 40 Gb/s. However, data rates as low as 0.2 on a scale of ω/ω_n would also exhibit low GD values, and that corresponds to the conditionally stable terms as in Fig 3. An input overload current of TIA is inversely proportional to the total absolute value of the feedback resistor even if it is of a nonlinear form. Having $R_{TIA} = 81$ k Ω puts the input current of 100 μ A within an acceptable range.

2. IFWM-Induced Noise Suppression

Before considering IFWM-induced noise, thermal characterization of the TIA amplifier was evaluated. Main thermal sources are “resistors” as well as Angelov and Statz transistor models. These components were set in simulated operation at 30°C. Parastic capacitances of the Angelov M_1 transistor model were as $C_{ds} = C_{gd} = 0.001$ pF, $C_{gs} = 0.1 C_{ds}$. As for the Statz M_2 model, $C_{ds} = C_{gd} = C_{gs} = 0.001$ pF.

When applying the IFWM-induced phase and amplitude noise to the TIA and following on Equation 8, a normalized form is presented. A two noise source currents were embedded as part of the TIA input (in simulation), one represents IFWM-induced amplitude noise and the other represents IFWM-induced phase noise respectively. Both of these

sources are taken to be the mean-square noise current spectral density (in pA²/Hz). A correlation coefficient that combines the two sources is defined as I_{12} defined in the Microwave Office program:

$$I_{12} = \frac{i_1 i_2^*}{\sqrt{i_1^2 i_2^2}} \dots\dots\dots(12)$$

Comparing the right hand sides of Equation 8 with Equation 12, we arrive at the following normalization:

$$i_1 \equiv \sum_{l,m \neq 0} \text{Re}\{AC_{l,m}\} \dots\dots\dots(13)$$

$$i_2^* \equiv \sum_{l,m \neq 0} \text{Im}\{AC_{l,m}\} \dots\dots\dots(14)$$

$$\frac{1}{\sqrt{i_1^2 i_2^2}} = E \dots\dots\dots(15)$$

where Equation 13 represents the IFWM-induced amplitude noise (real term) in optical fiber, while Equation 14 represents IFWM-induced phase noise as it is in an imaginary form, while the IFWM optical field amplitude is normalized in Equation 15.

Under pure thermal conditions of 30°C (*i.e* before applying any combined IFWM noise), circuit MNF (Minimum Noise Figure) value was 1.758 dB at 40 GHz using 81 kΩ nonlinear feedback resistor R_{TIA} , as in Fig 5. A 1.760 dB of MNF is registered when R_{TIA} value changes to 80 kΩ. The embedded IFWM optical power was taken to be 80.922 mW (within typical range of 60 mW – 120 mW). Having the amount of 80.922 mW to corresponds to 19.081 dB which was interpolated to a noise value of 8×10^{-18} pA/ $\sqrt{\text{Hz}}$ that represents the actual noise input. The IFWM-induced noise value of 19.081 dB is effectively suppressed under the influence of TIA input impedance Z_{in} of 19914 Ω (frequency domain) which leads to IFWM combined noise of 14.55 dB in a decreasing pattern at TIA output as in Fig 6. R_{TIA} had a considerable effect on thermal cancellation, but with little or no effect on IFWM-induced noise. Incidentally, the thermal conditions of 30°C during IFWM-induced noise simulated measurement still applied. It is the virtual ground node between $1/C_s$ and Z_{in} at 40 Gb/s by which the level of IFWM combined noise is suppressed. To be more precise, the value of R_2 in Fig 1 which is set at 863 kΩ that has the major dominating factor (within Z_{in}) to control the 5 dB reduction range of IFWM noise. Higher or lower than 863 kΩ values lead to IFWM noise reduction lower than 5 dB. The presence of R_{TIA} is only to optimize thermal noise and has nothing to do with IFWM noise control.

An assessment of S-parameters was obtained in which the TIA gain was established through $|S_{21}|$ and found to be 10.15 dB at 40 GHz given the thermal conditions of 30°C as in Fig 7. Beyond 40 GHz, there is a considerable drop in gain which suggest that this particular configuration is valid for a band that is in a matching pattern with both noise and TIA bandwidth. An extremely limited reflected signal at the TIA input is shown as in Fig 8.

There is a very limited value of $|S_{11}|$ at 40 GHz, despite the amount of 19914Ω which is the input impedance of the circuit as a twin T notch filter. Resemblance to real-time fabricated TIA design is also considered for which parasitic capacitances were taken into effect.

Without the TIA procedure described above, so far, there is still serious limitations for 40 Gb/s systems or even lower if what is required is to secure a bit error rate lower than 10^{-9} . IFWM and other nonlinear optical impairments are still considered to be big hurdles. Having several stages of chromatic dispersion compensation devices alongside the optical path is a tedious effort to say the least.

An optical modulation, of all forms, to tackle pulse timing jitter especially for 40 Gb/s systems can be replaced by modulating its optical power into a form of electric current. A worst case situation of simulating TIA circuit components at 30°C , gives plenty of room for real-time maximum detectable current capable of being converted into a voltage swing. The Angelov and Statz transistor models (with embedded parasitic capacitances) represent a better alternative for signal processing that can put an end to any compensation techniques.

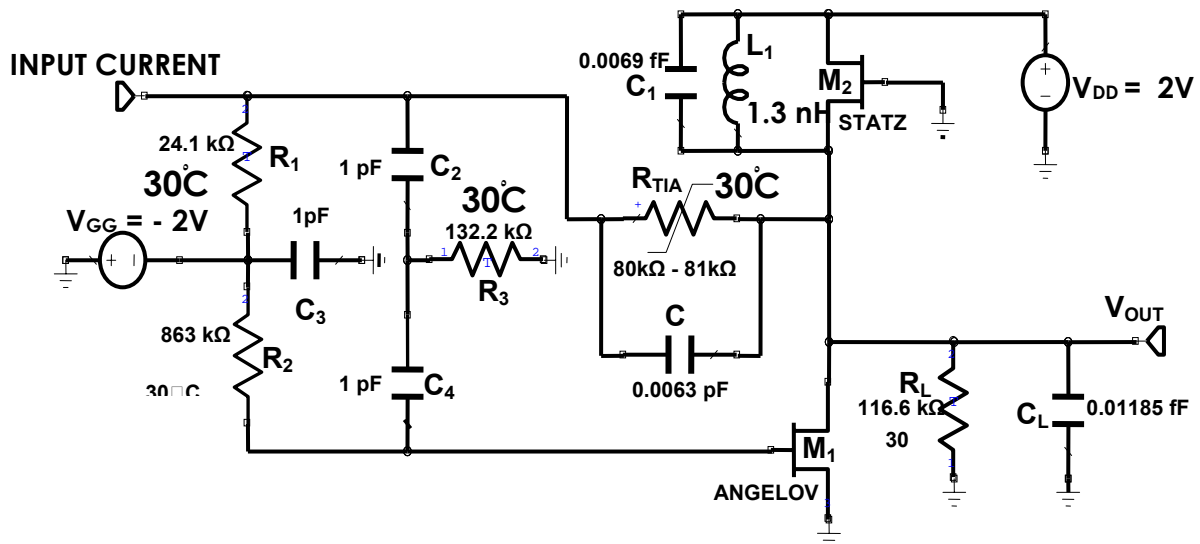


Fig. 1: Basic schematic of TIA circuit.

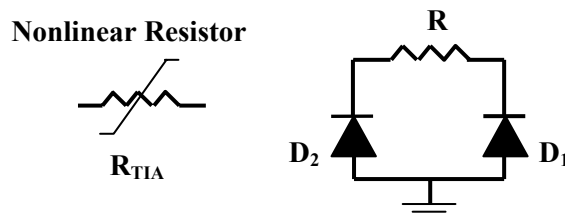


Fig. 2: Equivalent passive circuit of R_{TIA} .

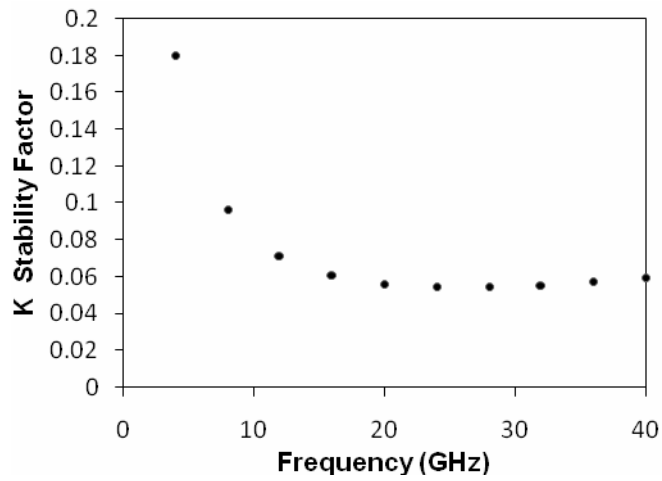


Fig. 3: 40 Gb/s stability factor performance.

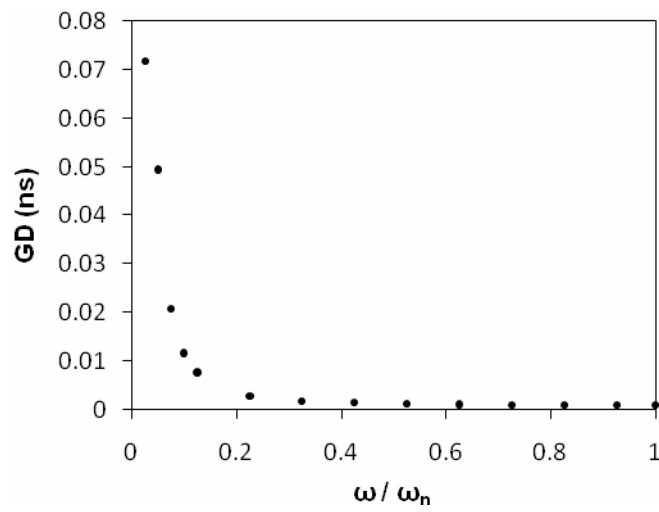


Fig. 4: TIA group delay is at minimum when $\omega = \omega_n$.

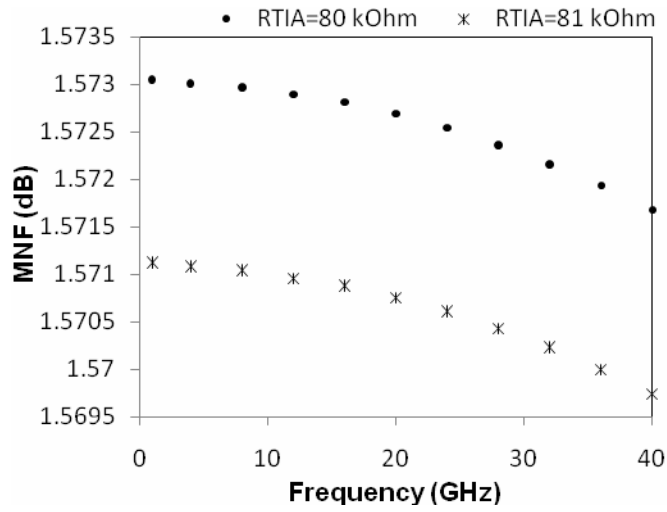


Fig. 5: Minimum Noise Fig (MNF) at temperature of 30°C (before applying Combined IFWM-induced noise) at $R_{TIA} = 80\text{ k}\Omega - 81\text{ k}\Omega$.

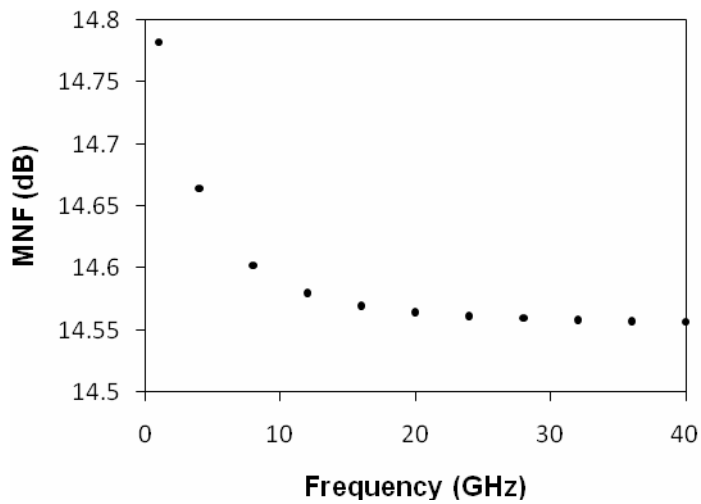


Fig. 6: Minimum Noise Fig (MNF) after applying IFWM-induced noise at $Z_{in} = 19914\ \Omega$ under thermal conditions of 30°C.

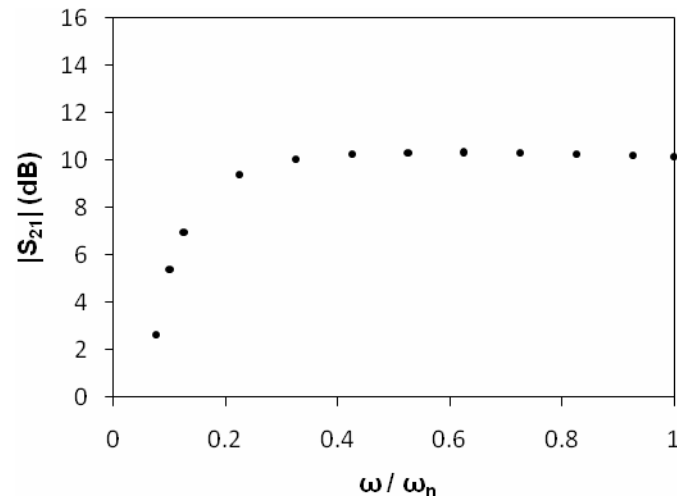


Fig. 7: $|S_{21}|$ versus frequency, a gain of 10.15 dB is reported at 40 Gb/s.

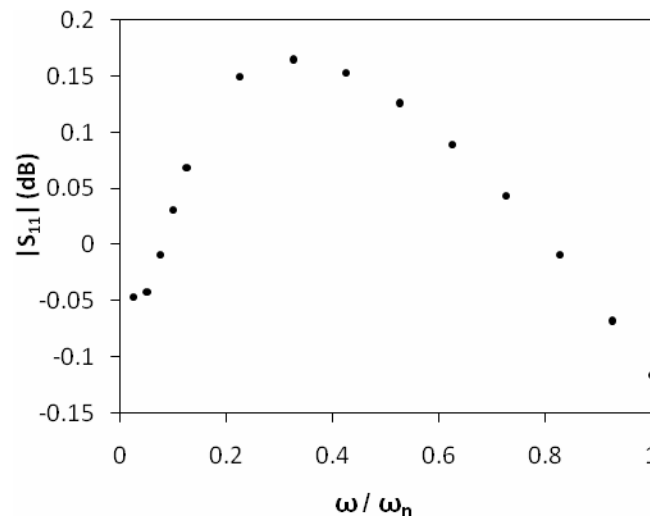


Fig. 8: $|S_{11}|$ of reflected signal showing a value of -0.13 dB at 40 Gb/s.

REFERENCES

- Agrawal, G. P. (2002). Fiber Optic Communication Systems, Chapter 3, New York, Wiley.
- Angelov, I.; Bengtsson, L. ; Garcia, M. (1996). Extensions of the Chalmers nonlinear HEMT and MESFET model, *IEEE Transactions on Micro. Theory and Techni.*, **44**, 1664-1674.
- Groenveld, D. J. A. (2010). Bandwidth Extension and Noise Cancelling for TIAs, M. Sc. Thesis, University of Twente, Twente, The Netherlands, pp. 17-34.

- Hirooka, T. ; Ablowitz, M. J. (2002). Suppression of intra-channel dispersion-managed pulse interaction by distributed amplification, *IEEE Photonics Technol. Lett.*, **14**(3), 316-318.
- Kumar, S.; Mauro, J. C.; Raghavan, S. ; Chowdury, D. Q. (2002). Intra-channel nonlinear penalties in dispersion-managed transmission systems, *IEEE J. Selected Topics in Quantum Electro.*, **8**(3), 626-631.
- Lau, A. P. T.; Rabbani, S. ; Khan, J. M. (2008). On the statistics of intra-channel four-wave mixing in phase-modulated systems, *OFC/NFOEC Conference on Optical Fiber Communication / National Fiber Optics Engineer Conference*, JThA, 52 p.
- Linghao, S. ; Takala, J. (2003). IFWM and IXPM Nonlinear Effects Suppression By Using Optical Pulse Position Modulation, *The 9th Asia-Pacific Conference on Communications APCC*, pp. 320-324.
- Mecozzi, A.; Clausen, C. B. ; Shtaif, M. (2000). Analysis of Intra-channel nonlinear effects in highly dispersed optical pulse transmission, *IEEE Photon. Technol. Lett.*, **12**, 392-394.
- Morita, I.; Suzuki, M.; Edagawa, N.; Tanaka, K. ; Yamamoto, S. (1999). Long-Haul soliton WDM transmission with periodic dispersion compensation and dispersion slope compensation, *J. Light Wave Technol.*, **17**(1), 80-85.
- Sackninger, E. (2005). "Broadband Circuits for Optical Fiber Communication". John Wiley and Sons, Hoboken, 130 p.
- Statz, H. (1987). GaAs FET Device and circuit simulation in spice, *IEEE Trans. Electron Devices*, ED-**34**, 160.
- Yamamoto, T.; Yoshida, E.; Tamura, K. R.; Yonenaga, K. ; Nakazawa, M. (2000). 640-Gb/s Optical TDM transmission-Over 92 km Through a Dispersion- Managed Fiber Consisting of Single-Mode Fiber and Reverse Dispersion Fiber. *IEEE Photonics Technol. Lett.*, **12**(3), 353-355.